

# Nonlinear interaction between two different photonic bandgaps of a hybrid photonic crystal fiber

Arismar Cerqueira S., Jr.,<sup>1,\*</sup> Cristiano M. B. Cordeiro,<sup>1</sup> F. Biancalana,<sup>2</sup> P. J. Roberts,<sup>3</sup>  
H. E. Hernandez-Figueroa,<sup>1</sup> and C. H. Brito Cruz<sup>1</sup>

<sup>1</sup>Optics and Photonics Research Center, Unicamp, 13083-970, Campinas Sao Paulo, Brazil

<sup>2</sup>Department of Physics and Astronomy, Cardiff University, Queen's Buildings, The Parade, CF24 3AA, Cardiff, UK

<sup>3</sup>Department of Photonics Engineering, Danish Technical University, DK-2800 Kongens Lyngby, Denmark

\*Corresponding author: arismar@dmo.fee.unicamp.br

Received June 10, 2008; revised July 31, 2008; accepted August 9, 2008;  
posted August 18, 2008 (Doc. ID 97269); published September 9, 2008

Nonlinear interaction between spectral components in two different photonic bandgaps is experimentally demonstrated by launching femtosecond pulses near a zero-dispersion wavelength of a hybrid photonic crystal fiber, which guides by a combination of total internal reflection and bandgap effects. It is demonstrated that the initial pulse becomes spectrally broadened, and narrowband resonant radiation is generated in a different bandgap from the one responsible for guiding at the pump wavelength. The spectral intensity of the resonant radiation peaks at 2.7 dB below that of the broadened pulse in the pump-guiding bandgap. © 2008 Optical Society of America

OCIS codes: 060.5295, 190.0190, 190.7110.

Photonic crystal fiber (PCF) technology provides efficient dispersion management that is extremely useful for nonlinear optics. The optical properties of PCFs are determined by the cladding photonic crystal and the core size. Hybrid photonic crystal fiber [1], see Fig. 1, is a novel type of PCF that guides by virtue of two propagation mechanisms simultaneously. Its structure is composed of air holes and germanium-doped silica rods arranged around an undoped silica core. Total internal reflection and anti-resonance effects [2], central to one-dimensional photonic bandgap (PBG) formation, act together to confine light within the guiding core. Light at wavelengths satisfying the antiresonant condition is guided in the pure silica core by antiresonant reflection from periodically placed high-index rods. Therefore, light is going to be guided in its core by index guiding in one direction and the by antiresonance effect in the other, even if the PBG structure is not a full two-dimensional photonic crystal structure.

The possibility of exploiting both propagation mechanisms enables nonlinear fiber optic experiments in new dispersion regimes. To illustrate this, a femtosecond system was used to perform nonlinear experiments using a hybrid PCF by launching light near one of its zero-dispersion wavelengths ( $\lambda_0$ ).

**Nonlinear experiment:** The hybrid PCF used in this paper is shown in Fig. 1, having air hole diameter  $d=1.59\ \mu\text{m}$ , interhole spacing  $\Lambda=3.85\ \mu\text{m}$ , germanium rod diameter  $D=3.75\ \mu\text{m}$ , and a gradient index with maximum step  $\Delta n=2.03\%$ . Figure 2(a) shows simulations of its confinement loss and chromatic dispersion. The fiber provides three transmission windows over the wavelength range shown. The first one suffers from very high confinement loss. On the other hand, the two shorter windows provide an acceptable confinement loss and constitute the PBG regions of relevance to this work, in which we are going to use

very short fiber lengths. A supercontinuum source was used to measure the spectrum transmitted through 1 m of the fiber, shown in Fig. 2(b). It constitutes two PBGs that closely correspond to the calculated transmission windows. The discrepancy between them is due to uncertainties in the fiber structural parameters. The second PBG is centered on 800 nm, and the third PBG is in the visible region around 600 nm. It is well known that PBG fibers provide one  $\lambda_0$  for each PBG [3]. We have demonstrated that dispersion in hybrid PCFs is a result of both propagation mechanisms, so it can be efficiently controlled to obtain a  $\lambda_0$  at an advantageous position inside each PBG [1]. The geometry was chosen to ensure that there is one  $\lambda_0$  in the wavelength range of our femtosecond system, which consists of a fiber-based optical parametric amplifier, producing 60 fs pulses at a 1 kHz repetition rate.

A pulse centered at 830 nm was coupled into 28 cm of hybrid PCF. By using a variable attenuator, the average power ( $P_{\text{in}}$ ) was controlled and varied between 10 and 240  $\mu\text{W}$ . Figure 3(b) shows the nonlinear behavior as a function of  $P_{\text{in}}$ . The initial pulse becomes

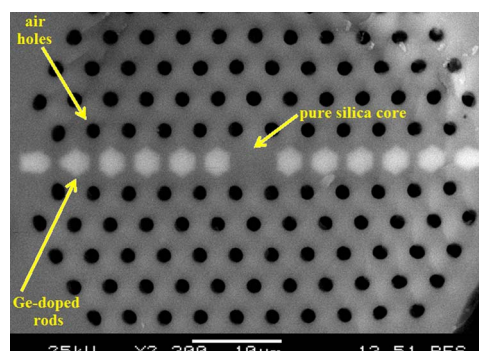


Fig. 1. (Color online) Hybrid PCF: the black circles are air holes and the white inclusions are Ge-doped rods.

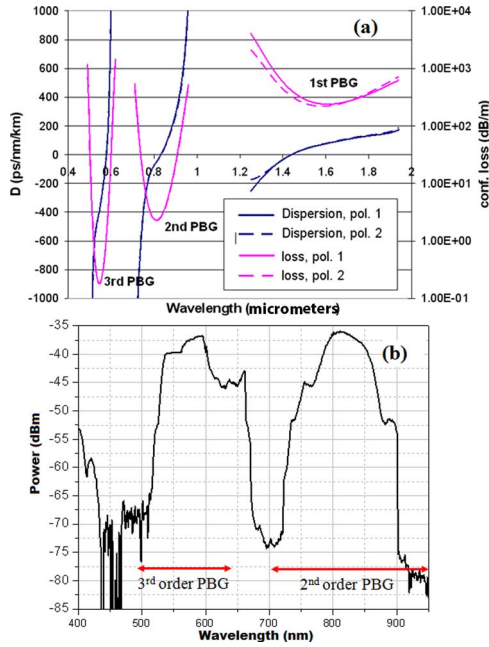


Fig. 2. (Color online) Hybrid PCF results: (a) Simulations of confinement loss and chromatic dispersion; (b) measured transmitted spectrum and the calculated 2nd and 3rd order PBGs shown in gray.

spectrally broadened, and above  $10 \mu\text{W}$  of input power we can see the appearance of resonant radiation (RR) that was emitted in the visible range by a soliton that is formed (slightly shifted by the Raman effect at about  $860 \text{ nm}$  [4]) from the input pulse. The soliton is situated in the second PBG, whereas the emitted dispersive radiation resides in the third PBG. This implies nonlinear interaction between spectral components within these bandgaps, which becomes efficient only when the radiation condition occurs. We will support these statements in the following with an analysis of both the radiation condition and the nonlinear output spectra in the third PBG.

The radiation condition between the soliton and the emitted radiation [5] is satisfied at a frequency  $\omega$  given approximately by  $k(\omega) = \gamma q$ , where  $k(\omega)$  is a moving-frame measure of the linear propagation constant at frequency  $\omega$  compared with its value at the soliton central frequency in the second PBG,  $\gamma$  is the nonlinear coefficient, and  $q = I/2$ , with  $I$  the soliton intensity. We estimated the nonlinear coefficient, tak-

ing into account the simulated effective area, in  $\gamma = 7 \text{ W}^{-1} \text{ km}^{-1}$ .  $k(\omega)$  is expanded up to the third-order dispersion term:  $k(\omega) = \beta_2 \Delta\omega^2/2 + \beta_3 \Delta\omega^3/6$  where  $\Delta\omega = \omega - \omega_0$  with  $\omega_0$  the soliton central frequency. The solitonic regime corresponds to  $\beta_2 < 0$ , and in the absence of third-order dispersion, there cannot be any emission of RR. However, if  $\beta_3$  is positive and nonvanishing, the perturbation introduced is sufficiently strong to stimulate the emission at specific wavelengths, calculated using the above formula. See Fig. 3(a) for simulations of the radiation condition based on the nonlinear Schrödinger equation using calculated dispersion and mode effective area data. PBGs of interest are indicated approximately by the gray areas. These simulations give good qualitative agreement with experimental observations of the output spectra in the third PBG shown in Fig. 3(b). Resonant frequencies are given by the intersections between  $\gamma q$  and  $k(\lambda)$  and are indicated with gray dots for three different input powers: A, B, and C correspond to  $1$ ,  $30$ , and  $100 \mu\text{W}$ , respectively. The resonant frequency is slightly shifted toward shorter wavelengths when the input soliton  $P_{\text{in}}$  increases. This clearly indicates that a soliton is formed in the second PBG and that the radiation observed in the third PBG is RR.

The radiation condition depends only on the dispersion of the second PBG, where the soliton is launched. Although a resonant dispersive wave emitted from a soliton has also been observed in PBG fibers filled with liquids [6], the most interesting and unique feature of our work is that the radiation condition occurs between two different bandgaps at widely separated wavelengths. The RR is created in the normal dispersion region of the third PBG, whereas the soliton is in the anomalous dispersion region of the second PBG. The strong RR obtained in the visible range demonstrates that the soliton is launched very close to the one  $\lambda_0$ , owing to the exponential sensitivity of the radiation's intensity to its spectral detuning with the soliton [5]. When an intense ultrashort pulse propagates near  $\lambda_0$  of an optical fiber, the input spectrum evolves into two well-separated components. When  $\beta_2$  is small, the pulse experiences strong self-phase modulation, which broadens its spectrum. Higher-order dispersion terms are significant, so as the pulse bandwidth broadens, different parts of the spectrum experience different  $\beta_2$ . When  $\beta_3$  is the dominant term, opposite sides of the pulse spectrum experience normal or anomalous  $\beta_2$ . On the anomalous side, the pulse spectrum continues to broaden until  $\beta_2$  becomes large enough to roughly balance self-phase modulation, at which point we obtain a stable soliton with a pronounced shift in center frequency. Spectral components of the soliton tail are in resonance with a dispersive wave.

Figure 4 presents an experimental analysis of the nonlinear response as a function of the pump central wavelength ( $\lambda_c$ ). As expected, the longer  $\lambda_c$ , the shorter the central RR wavelength. This is because as  $\lambda_c$  moves further from  $\lambda_0$ , at approximately  $820 \text{ nm}$  [Fig. 2(a)],  $\beta_2$  increases relative to  $\beta_3$ , and the

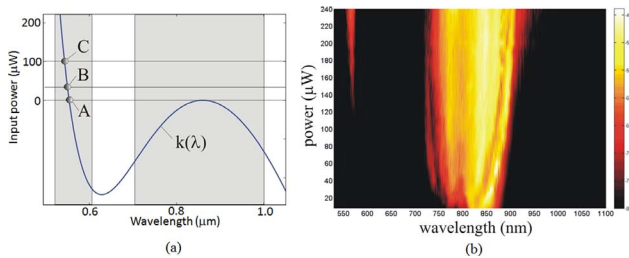


Fig. 3. (Color online) Nonlinear analysis as a function of input power: (a) Radiation condition curve between soliton wavenumber and radiation; (b) Measured output spectrum of pump and RR.

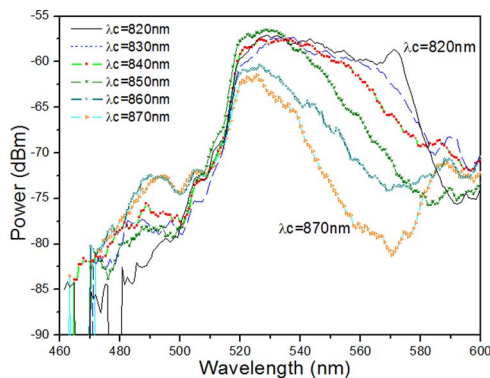


Fig. 4. (Color online) Nonlinear response as a function of pump central wavelength.

radiation condition involving  $k(\omega)$  requires a shift to shorter wavelengths.

Figure 5 shows an experimental result obtained by launching a pulse centered at 830 nm into 28 cm of Hybrid PCF at  $P_{in}=120 \mu\text{W}$ . It gave the most efficient excitation of RR, in which the spectral intensity of the RR peaks at 2.7 dB below that of the broadened pulse in the pump-guiding PBG. This improvement was achieved by optimizing the pulse polarization at the fiber input. The Ge inclusions produce a significant stress field, and since they are positioned along a line through the structure, they give rise to

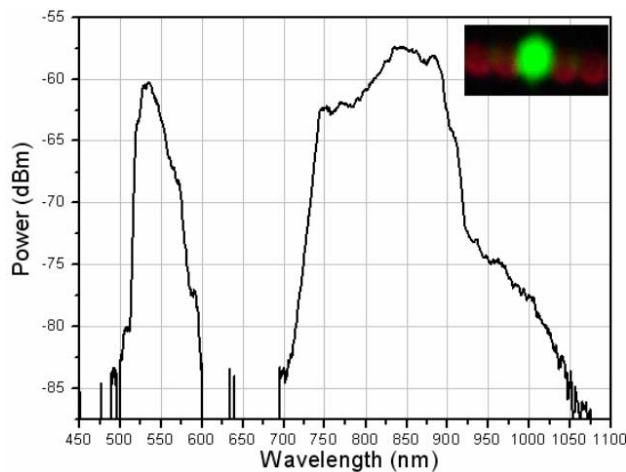


Fig. 5. (Color online) The most efficient RR excitation case and a photograph of green light at the fiber output.

an asymmetric stress field within the core that induces a sizeable birefringence [7]. The asymmetric stress distribution will split the two polarization modes and cause a polarization-dependent loss. Calculations of stress birefringence effects will form the basis of a future work. The inset of Fig. 5 shows that the infrared light was converted to green light in the PCF core.

We have observed, for the first time to our knowledge, nonlinear interaction and wavelength conversion between two different bandgaps. The initial pulse becomes broadened, and RR emitted by a soliton is observed in the visible range (green light). The soliton is situated in the second PBG, whereas the dispersive radiation lies in the third PBG. The spectral intensity of the resonant radiation peaks at 2.7 dB below that of the broadened pulse in the pump-guiding PBG. Hybrid PCFS are appropriate for experiments in nonlinear fiber optics in new dispersion regimes.

The authors thank J. Knight and A. George for help in fabricating the fiber and K. Z. Nobrega for the fruitful discussions. The authors from Brazil acknowledge FAPESP (Fundação de Amparo à Pesquisa e ao Ensino do Estado de São Paulo) for financial support. The work at the Danish Technical University was supported by the Danish High Technology Foundation.

## References

1. A. Cerqueira S. Jr., F. Luan, C. M. B. Cordeiro, A. K. George, and J. C. Knight, *Opt. Express* **14**, 926 (2006).
2. N. M. Litchinitser, S. C. Dunn, P. E. Steinvurzel, B. J. Eggleton, T. P. White, R. C. McPhedran, and C. M. Sterke, *Opt. Express* **12**, 1540 (2004).
3. J. Jasapara, T. H. Her, R. Bise, R. Windeler, and D. J. Digiovanni, *J. Opt. Soc. Am. B* **20**, 1611 (2003).
4. F. Biancalana, D. V. Skryabin, and A. V. Yulin, *Phys. Rev. E* **70**, 016615 (2004).
5. N. Akhmediev and M. Karlsson, *Phys. Rev. A* **51**, 2602 (1995).
6. A. Fuerbach, P. Steinvurzel, J. Bolger, and B. Eggleton, *Opt. Express* **13**, 2977 (2005).
7. T. Schreiber, F. Röser, O. Schmidt, J. Limpert, R. Iliew, F. Lederer, A. Petersson, C. Jacobsen, K. Hansen, J. Broeng, and A. Tünnermann, *Opt. Express* **13**, 7621 (2005).